ESCUELA TÉCNICA SUPERIOR DE INGENIEROS INDUSTRIALES Y DE TELECOMUNICACIÓN

INGENIERO TÉCNICO DE TELECOMUNICACIÓN, ESPECIALIDAD EN SONIDO E IMAGEN

Thesis title:

A MULTIRESOLUTION METHOD FOR INTERNAL WAVE DETECTION AND COLOR DISPLAY FROM SATELLITE IMAGES

Student: Erkuden Goikoetxea Basilio

Tutor: Doctor Ingeniero Industrial Luis Serrano Arriezu

ABSTRACT

In the present work an algorithm for wave detection is developed. The followed methodology is based on the multiresolution processing , the wavelet transform and the RGB model

This algorithm has been tested in three SAR images provided by the COSMO-Skymed satellite from the ASI.

First, Gaussian masks are generated in order to detect edges in the horizontal and vertical directions. This work is repeated in four resolution levels. Each level depends on the size and the variance of the gaussian mask. Once the horizontal and vertical edges are found, it is followed a non-maximal supresion processing to discard not relevant edges. This images are enhanced by morpfological processing. To integrate the levels into a single image in order to interpretate the obtained results it is used the RGB model. Each one of the first three levels is introduced in a RGB image channel. Finally the pixels that appear in white are the corresponding to the most important edges, that is the waves.

In the framework of ERASMUS Program, this work has been developed and completed at the Department of Biophysical and Electronic Engineering (DIBE) of University of Genoa (Italy), where the student has spent a period of about 11 months (starting from September 2010, to July 2011).

The satellite images used in the present work have been provided by the pilot project “OPERA (Operational Evaluation Of Damages In Flooded Areas Combining Cosmo-Skymed And Multispectral Optical Images) – Civil protection from floods” [*] funded by the Italian Space Agency in cooperation with the Italian Department for Civil Protection.

[*] E. Angiati, G. Boni, L. Candela, F. Castelli, S. Dellepiane, F. Delogu, F. Pintus, R. Rudari, S. B. Serpico, S. Traverso, and C. Versace, “Operational Evaluation Of Damages In Flooded Areas Combining Cosmo-Skymed And Multispectral Optical Images”, *IGARSS 2010, IEEE Geoscience and Remote Sensing Symposium*, pp. 2414-2417, July 2010.

INDEX

1 INTRODUCTION

Internal waves are an important ocean mesoscale phenomenon characterized by large energies. They have a destructive power with the buildings on the ocean, for examples, marine petroleum platforms. The safety of ocean navigation is obstructed, and acoustic propagation courses are disturbed. For these reasons the change of internal waves are widely followed by scientists of different work areas. In the past, the ocean internal wave fields have been measured by instruments like temperature and salinity sensors or current meters or by acoustic instruments like sonar [Ref Lee-Lueng Fu Benjamin].

With the development of remote sensing field, the manifestation of internal wave can be captured by a variety of remote sensing instruments, e.g., by ship radar, ground-based radar and photographic camera and airborne radar imaging.

Mollo-Christensen and Mascarenhas (1 979) demonstrated that satellite-derived information on these waves can be used to map the heat content in the upper ocean, thus making this information important in modelling the climate of coastal areas. How significant the generation of these waves is in draining the tidal energy is also an interesting question for tide modellers.

The manifestation of internal wave packets on SAR ocean images has always been of considerable interest for oceanographers. SAR images have great characteristics in relation to ocean monitoring.

The image characteristics and quality parameters that are most important for a qualitative interpretation of the SAR imagery of the ocean surface are discussed below.

For a SAR system, backscatter from the ocean surface is produced predominantly by the Bragg resonant scattering mechanism (e.g., Valenzuela, 1978). That is, the surface waves travelling in the radar range direction with a wavelength of $\lambda / 2\sin(\theta)$, the “Bragg resonant waves,” account for most of the backscattering, where λ is the radar wavelength and θ the incidence angle. What the SAR sees

on the ocean surface is primarily the variation of these waves [Ref Lee-Lueng Fu Benjamin]. Therefore, any phenomenon able to produce modulation in these waves is presumably detectable by the SAR.

In this project it is proposed an internal wave detection method in SAR satellite images. To reach this goal it is chosen a technique based on the multiresolution processing and the wavelet transform.

In the last decades, the scientists have studied the oceanographic features like the wind speed, ocean bottom tomography and others. In this study, we have been working just on the SAR images without taking into account any external data.

The original images will be studied in four different levels, each one corresponding to a different size of neighbourhood. In order to process the images with this multiresolution method, Gaussian masks are created in four levels. To obtain the Wavelet Transform, the partial derivatives of the previous Gaussian masks will be used. Once the four wavelet transforms are found, the gradient maxima are searched using the non-maximal suppression method. That is, the modulus and the phase will be calculated and then, the pixels with a local maximum along the direction indicated the phase are found. Finally, a single RGB image will be represented in which the internal waves will be visible.

The general methodology explained before could be used to detect any edge in all type of images.

In Chapter number two, an overview of SAR images and an explanation of the characteristics of the ocean waves will be expounded. In the SOA section, there will be shown the relevant algorithms of the last decades about internal waves detection. In later chapters, the detailed methodology of the work and its intermediate results will be discussed. In the conclusions, the method is evaluated and the further investigations are presented.

2 Ocean SAR images: formation and characteristics

2.1 Introduction

The most utilized instrument in the last decades to get ocean features information, such as ocean waves, tidal currents, ship routing, etc, in a quickly way has been the SAR (Synthetic Aperture Radar). With a SAR system it is possible to obtain images of the illuminated ground location in almost any weather condition (sun, rain, fog) and illumination condition (day or night).
SAR systems have been mounted on aircrafts, spacecrafts and satellites such as ERS, ENVISAT, COSMO-SkyMed and TERRASAR-X.

2.2 SAR images

The SAR is an imaging radar technique that achieves high resolution by mounting on a moving platform (aircraft or spacecraft), an antenna from which a target scene is repeatedly illuminated with microwaves. [Ref Lee-Lueng Fu Benjamin]
The SAR is generally able to transmit several hundred pulses while its parent spacecraft passes over a particular object. Many backscattered radar responses are therefore obtained for that object.
After intensive signal processing, all of those responses can be manipulated such that the resulting image looks like the data were obtained from a big, stationary antenna.

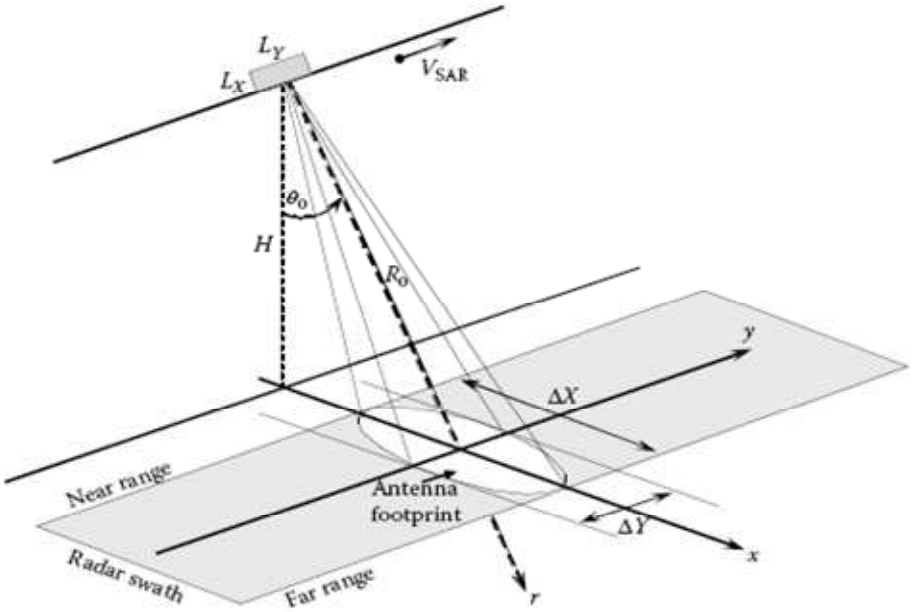

Fig 2.2.1 SAR system geometrical configuration

The synthetic aperture stands for the distance traveled by the platform while the radar antenna is collecting information about the target.

Aperture is simply the radar antenna length: a very long antenna is synthesized by moving a small one along the flight path.

The aim of the processing is to use the data received by the antenna from the many pulses reflected by each single target to reconstruct the best representation of the 2-D reflectivity function.

The SAR images which have been used in this project are 2-D arrays of pixels where one of them is associated to a small area of the Earth's surface whose size depends on the SAR system characteristics.

2.3. Oceanographic phenomena from a SAR system

Subsurface hydrodynamic phenomena (such as internal waves, internal tides, tidal currents, and eddies) interact through complex processes with the surface field. There are many diverse areas where information on subsurface hydrodynamic phenomena would be of great interest, including off-shore drilling and mining, ship routing, fisheries, aqua culture, environmental monitoring, acoustic communication, and coastal engineering. Knowledge of wave conditions, on either an historical or real-time basis, assists such a particular area of interest by reducing the costs and improving the safety of many operations. [Ref Rodenas, Garello].

It is generally believed that internal waves are seen by a radar and/or a camera mainly as a result of either or both of two mechanisms: On the one hand, the surface currents associated with the internal wave field sweep together surface oils and materials in the surface water convergence zones, resulting in severe damping of short capillary/gravity waves to form slicks (Ewing, 1950); and in the other hand the interaction of the short capillary/gravity waves and the surface current field induced by the internal waves results in a periodic modulation in the height of the capillary/ gravity waves, thus producing the banded patterns of roughness and slicks with occasional occurrence of highly peaked, long-crested waves that are the result of resonant interactions.

Characteristics of the internal waves can be summarized as follows [Ref Lee-Lueng Fu Benjamin Holt]:

At first, most of these waves are found in coastal areas with wave crests more or less parallel to the bottom topography. Besides, these waves generally propagate onto the shores in separate groups with the distance between groups ranging from about 10 to 60 kilometres. The wavelength within each group decreases monotonously from several kilometres at the leading edge to several hundred meters at the trailing edge. The crests range in length from about 10 to 100

kilometres and are characterized by either narrow bright lines in a dark background or by relatively wider dark lines in a bright background, indicating that these waves can be detected at a substantial range of wind speed.

One of the problems in detecting internal wave signatures on the ocean surface using satellite SAR images lies in distinguishing internal waves from other oceanographic and SAR phenomena. Internal wave lookalike effects may include natural film, greasier, threshold wind speed areas, wind sheltering by land, rain cells, current shear zones, oil slicks, eddies ships and ship wakes, and upwelling. Among this look-alike effects, natural film, rain cell, and current shears have been see to represent the major problem. [Ref Rodenas,Garello]

Often, the internal wave groups are created by the bottom topography of the ocean, and they are usually represented simultaneously with a bathymetric char of the area as is it shown in the Fig 2.3.1.

The goal of the present study is to develop a method for internal wave detection.

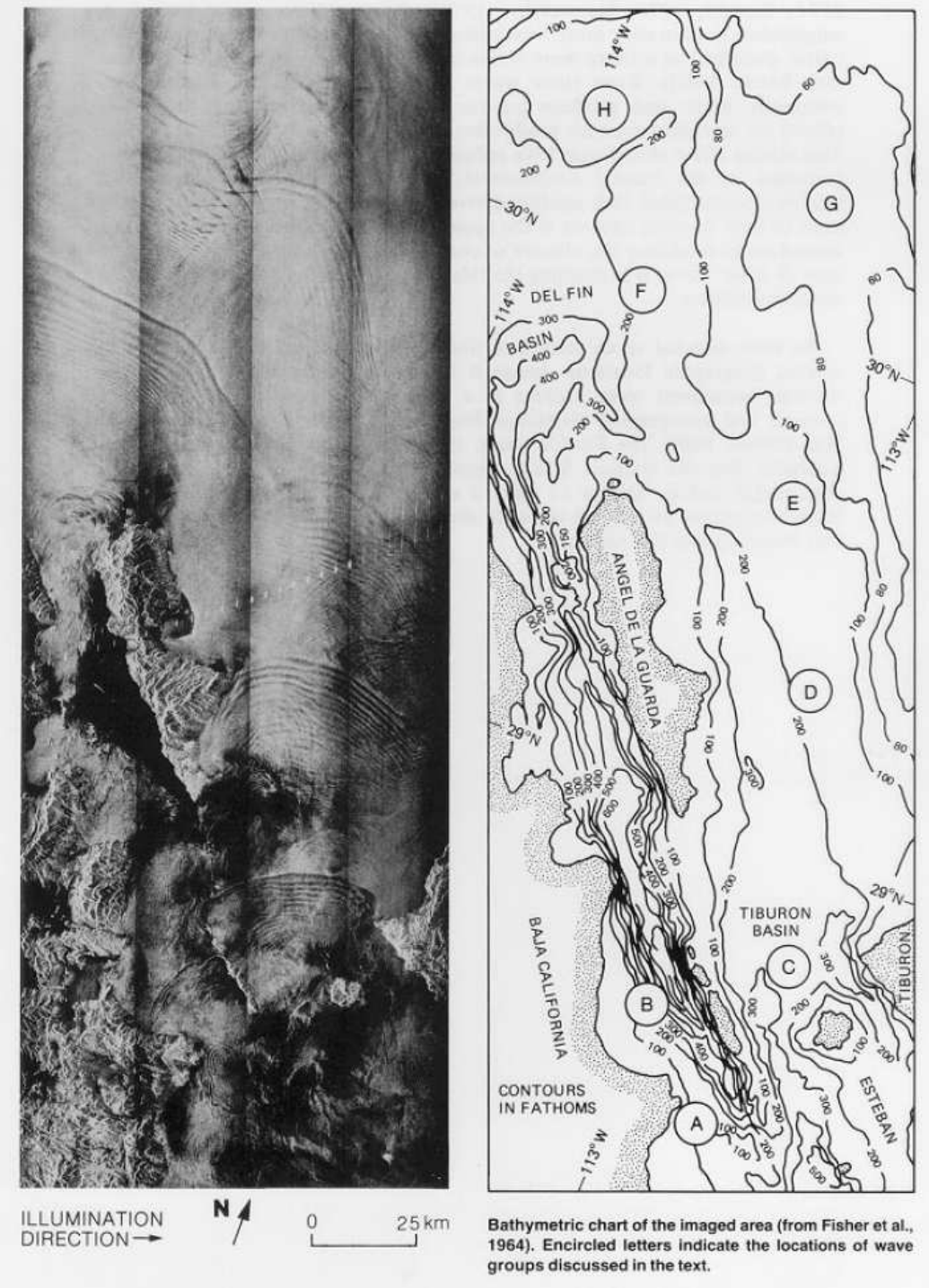

Bathymetric chart of the imaged area (from Fisher et al., 1964). Encircled letters indicate the locations of wave groups discussed in the text.

Figure 2.3.1. Seasat image of the Gulf of California and its internal waves and the corresponding bathymetri chart of the area. [Ref
Lee-Lueng Fu Benjamin Holt]:]

3 STATE OF ART:

3.1 Seasat and overview of wave detection methods

Seasat, the first satellite dedicated to the use of microwave sensors for observation of the Earth's oceans, was launched on June 28, 1978, by the United States National Aeronautics and Space Administration; The project was managed by the Jet Propulsion Laboratory (JPL) of the California Institute of Technology.

The JPL published the work after the Seasat mission, in that research it is performed a study of the ocean features such as surface waves, internal waves and ship wakes using the Seasat images to explain them all. Moreover, a characterization of the tidal currents and internal waves of the American coasts is explained. [Ref Lee-Lueng Fu Benjamin Holt]:

Since that mission, much knowledge has been gained on the potential of synthetic aperture radar technology in oceanography.

There have been several researches about the detection of internal waves using different methods such as, wavelet transform, Fourier transform, the Radon transform etc.

In this section there will be explained the most important methods about the detection of internal waves that have been studied.

3.2 A Wavelet Localized Radon Transform Based Detector for a Signal with Unknown Parameters

In the paper, a new transform which combines the key features of the Radon transform and the wavelet transform is presented. This transform, developed as a response to the problem of wake detection on open water SAR images, has parameters for rotation in addition to spatial localization. Images with arbitrary

positioned linear features are shown to produce strong horizontal lines on the transformed domain. This property is used to construct a wavelet localized Radon transform based detector.

This approach is based on the problem of wake detection in the open ocean. That problem is extremely difficult for several reasons. First, although some information about the shape of the wake is known a priori, the actual location of the wake is not known. In addition, often the wake is present in a significant amount of noise. In order to find a useful detection scheme, several mathematical techniques have been studied including the Radon transform and the wavelet transform.

The Radon transform, which emphasizes linear features, has proven useful in the wake detection problem. However, because the transform does not have inherent localization properties, the Radon transform is not useful on arbitrary open water wake images. In order to combat this problem, various techniques including additional processing on the image and localizing the Radon transform have been considered.

Unlike the Radon transform, the wavelet transform naturally has space scale localization. The wavelet transform has been successfully used in the wake detection problem, when the location of the wake was known a priori. However, the standard two dimensional wavelet transform does not have parameters that easily identify the location of the linear feature. **A** new transform which combines the key features of the Radon transform with the localization abilities of the wavelet transform is presented.

The main problem is the inverse problem, i.e., reconstructing an image from its projections. The idea is to reconstruct an image which has a fine resolution in the area of interest, and a coarser resolution in the areas that are not of interest. In that paper, they consider the forward problem. In particular, they examine an image in the transform domain, where the transform is specially suited to emphasize arbitrarily positioned linear features. This representation is used to create a useful

detector, even when the exact position of the signal is not known a priori. [Ref Warrick, Delaney]

3.3 Internal Wave Detection and Location in SAR Images using Wavelet Transform

The algorithm presented by Rodenas and Garello is the one I have chosen to implement in this project. In this section an overview of the paper will be shown, therefore in the methodology section the details will be perfectly explained.
The goal of the paper of Rodenas and Garello is to develop an automatic method for internal wave detection and orientation in which dark spots with a high probability of being an internal wave are automatically identified. The first problem in the detection system is to distinguish sea from land in the **SAR** image.
The second problem is to detect the significant internal wave structures using a multiresolution processing and the wavelet transform. The wavelet transform gives spectral decomposition via the scale concept. By decomposing signals into elementary building blocks that are well localized both in space and frequency, the wavelet transform can characterize the local regularity of signals such as i.e. internal waves via the study of the local modulus maxima across decomposition scales. The 2-D wavelet transform is a highly efficient bandpass filter, which can be used to separate various scale processes and to show their relative phase/location information. [Ref Rodenas, Garello].

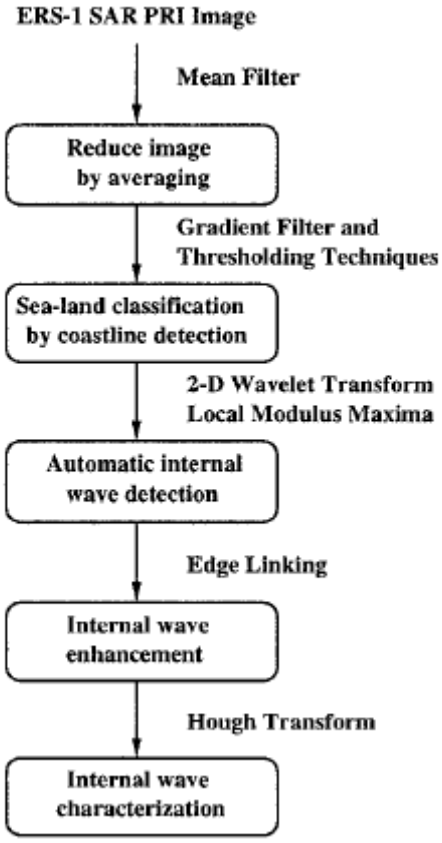

Figure 3.3.1 Block diagram given by Rodenas and Garello.

3.4 Satellite SAR Remote Sensing of ocean internal waves

In order to detect and extract the internal wave's characteristics in this paper are followed the next steps:

-Speckle noise of SAR images is suppressed with new filters that select Kaiser, Hamuring, Hunning and other windows as well as wavelet transform etc to get ocean internal wave SAR images with internal wave signatures.

-To extract the characteristic parameters of internal waves from SAR sub images it is used the two-dimensional Fast Fourier transform (2D-FFT).

-Geographical parameters can be determined according to spectrum features of internal waves.
-Studying the features of internal wave by wavelet transform method, it is proved that wavelet analysis method is better than FFT.
- The mean wavelengths of internal wave are estimated using wavelet analysis.
[Ref Zhou Changbao, Yang Jingsong, Huang Weigen, Fu Bin,Shi Aiqin, Li Donglin]

3.5. Internal Wave Detection and Wavelength Estimation

The aim of this study is to model internal wave speed, direction and wavelength. The utility of wavelet analysis is examined using two dimensional (2-D) wavelet transform for internal wave detection and wavelength estimation. The continuous wavelet transforms is also used to estimate energies and wavelengths within soliton peaks from the detected internal wave. The Doppler radar was used to estimate the speed of the internal wave. The results show that the wavelengths of internal wave are ranged from 30 m to 400 m.
It can be concluded that the integration between wavelet transform and Doppler model is an excellent tool to detect internal wave and the polarised L-band is more suitable for detection of internal waves compared to C-band. [Ref Marghany 1999].

3.6. Digital elevation model of internal wave detection

The main objective of the presented study is to introduce a new tool for internal wave detection as the internal wave has a lineament or curvilinear features in radar image. This tool will be based on the integration between digital elevation model and Canny algorithm.

The digital elevation model was applied with Canny algorithm to automatic detection of internal wave on the coastal waters of Kuala Terengganu, Malaysia. The continuous wavelet transform is used to estimate energy and wavelengths within soliton peaks from the detected internal wave. The Doppler radar was used to model the speed of internal wave.

This study shows that tidal spectra in South China Sea could generate the internal wave. The statistical analysis shows that polarized LHH band is more sensitive to detect the internal wave compared to LVV and CVV bands. The results obtained from TOPSAR polarized data are similar to ground isothermal profile.

It can be concluded that the integration between digital elevation model and Canny Algorithm could be used as automatic tools for internal wave detection. The isothermal profile of internal wave suggested that the irregular bottom topography and tidal flow are the main reason for the generation of internal wave in South China Sea. [Ref Marghany 2000].

3.7. Detection of ocean wave groupiness from spaceborne synthetic aperture radar

It is well known that ocean gravity waves form wave groups. These groups are observed as sequences of high waves with nearly equal periods, or wavelengths. Wave groups are often responsible for serious damages to marine systems (i.e., ships, off and onshore structures, etc.) when the period of the individual waves in the group are close to the resonance period of the system.

In the work, two methods to analyze wave groupiness in the spatial domain from sea surface images are presented: The first method is based on the two-dimensional generalization of the Smoothed Instantaneous Wave Energy History (SIWEH) function, which had been originally developed to analyze wave groupiness for wave elevation time series. The second method uses the estimation

of the wave envelope in two dimensions to extract wave grouping parameters. Assuming that the wave fields are Gaussian stochastic processes, both methods are applied to ERS-2 SAR and ENVISAT advanced SAR (ASAR) images of the sea surface, where only cases with almost range travelling waves are considered in order to avoid strong nonlinearities in the SAR imaging mechanisms. [Ref J. C. Nieto Borge, S. Lehner, A. Niedermeier and J. Schulz-Stellenfleth]

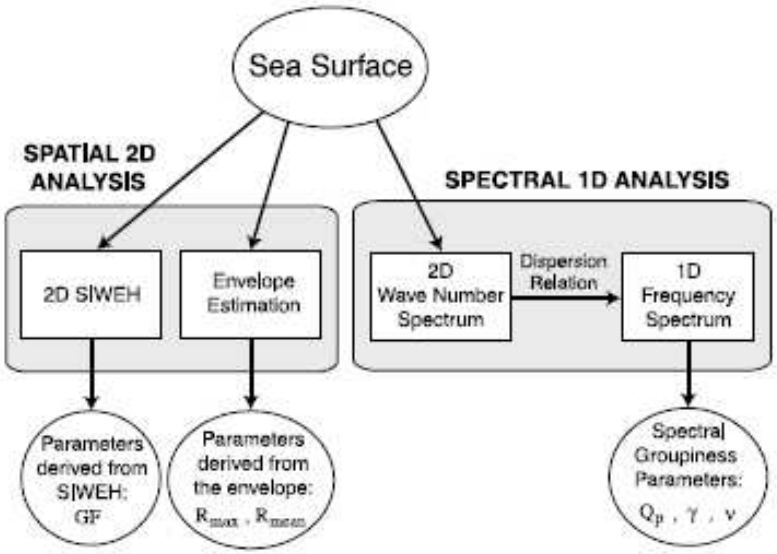

Figure 3.7.1 Block diagram of the Nieto's research.

3.8 Research on Detection of Internal Wave Area Based on Power Spectrum in SAR Image

One of the most popular processing in order to reach this goal is based on the well-known Fourier Transform and the Power Spectrum.

In the article it is developed the idea that ocean waves, internal waves, and islands have different character in SAR image, which is the power spectrum. They get

power spectrum character of different texture character in SAR image by Fourier transform, and conclude the specific power spectrum characters of internal wave. As a result, the method can be applied indetecting internal wave area.

As it was commented before in a SAR surface image, internal waves appear as long, bright and dark strips with a certain radian. In this article circular spectrum is adopted to transform the 2-D spectrum of SAR image into 1-D form and the method which is based on the unity energy spectrum is put forward to analyze the image spectrum characteristics. It supplies an effective method for detection of ocean internal waves. [Ref Biao Chen 1, Can Ding 2, Hai-ping Hou].

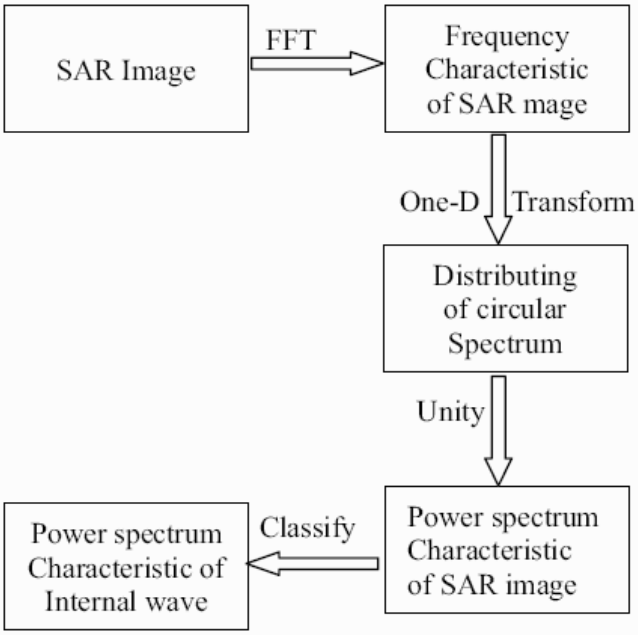

Figure 3.8.1. Block-diagram of the analysis of the power spectrum characteristics.

3.9 Evaluation and choice of the method

The main difference between the algorithms explained in this section, consists in their simplicity. Those which make use of the Fourier Transform method and of the spectrum are the least robust as it has been proved in the 3.4 section. This is the simplest method. Then, almost all the algorithms use the Wavelet Transform as it has the important property of locating the found frequencies. The Doppler analysis is used to find the speed of the wave and it is not the objective of this paper, therefore this method will not be used. One of the most versatile algorithms would be the one in which it is combined the Radon Transforms and the Wavelet Transform. I have not chosen this type of processing because of the fact that it would take me too much time to develop it, and it exceeds the aim of a three year carrier final project.

Finally, as it has been previously commented, the methodology used to reach the goal of this project is the Rodenas and Garello paper called *Internal Wave Detection and Location in SAR Images using Wavelet Transform*.

Among all the articles I have read and studied I have chosen that one because its methodology was the clearest and the most intuitive to implement allowing to achieve good results at the same time. The algorithm is explained using various examples, this way it is possible to know what kind of final image we want to reach. Besides, it gives me the chance to start learning about multiresolution processing and wavelets. As it is explained in the previous sections, the wavelet analysis is the most popular and it works better than the classical Fourier analysis in the field of the detection of internal waves.

4) METHOD:

4.1 Methodology architecture

The proposed method detects the internal waves after a multiscale processing in a SAR image. The first part of the algorithm is based on the Rodenas and Garello paper [Ref Rodenas, Garello].

The technique is based on a multiscale edge representation of images, specifically in the multiscale gradient maxima, originally developed by Mallat and Zhong.

The architecture of the method (Figure 4.1.1) is developed following the next steps:

- *Sea-land separation:* In this part it is necessary to get a binary mask that separates the sea from land.
- *Wavelets creation:* the creation of the wavelets is part of the off line processing, it is only used only at the beginning. The wavelets or masks to detect the edges have been obtained by using Gaussian vectors. Two masks for each level are used, each mask in a different direction. The size of the masks and the variance of them will be very important parameters for the later results.
- *Wavelet transform:* the wavelets calculated above are convolved with the original image to get the wavelet transform. It will have two components, one on the *x* direction and the other in the *y* direction.
- *Local modulus maxima extraction:* Similary as it is done in the Canny algorithm the modulus maxima of the wavelet transform images along the direction of the gradient will be found.
- *Fusion of the scales:* to integrate the information contained in the different resolution levels the RGB image model have been used.

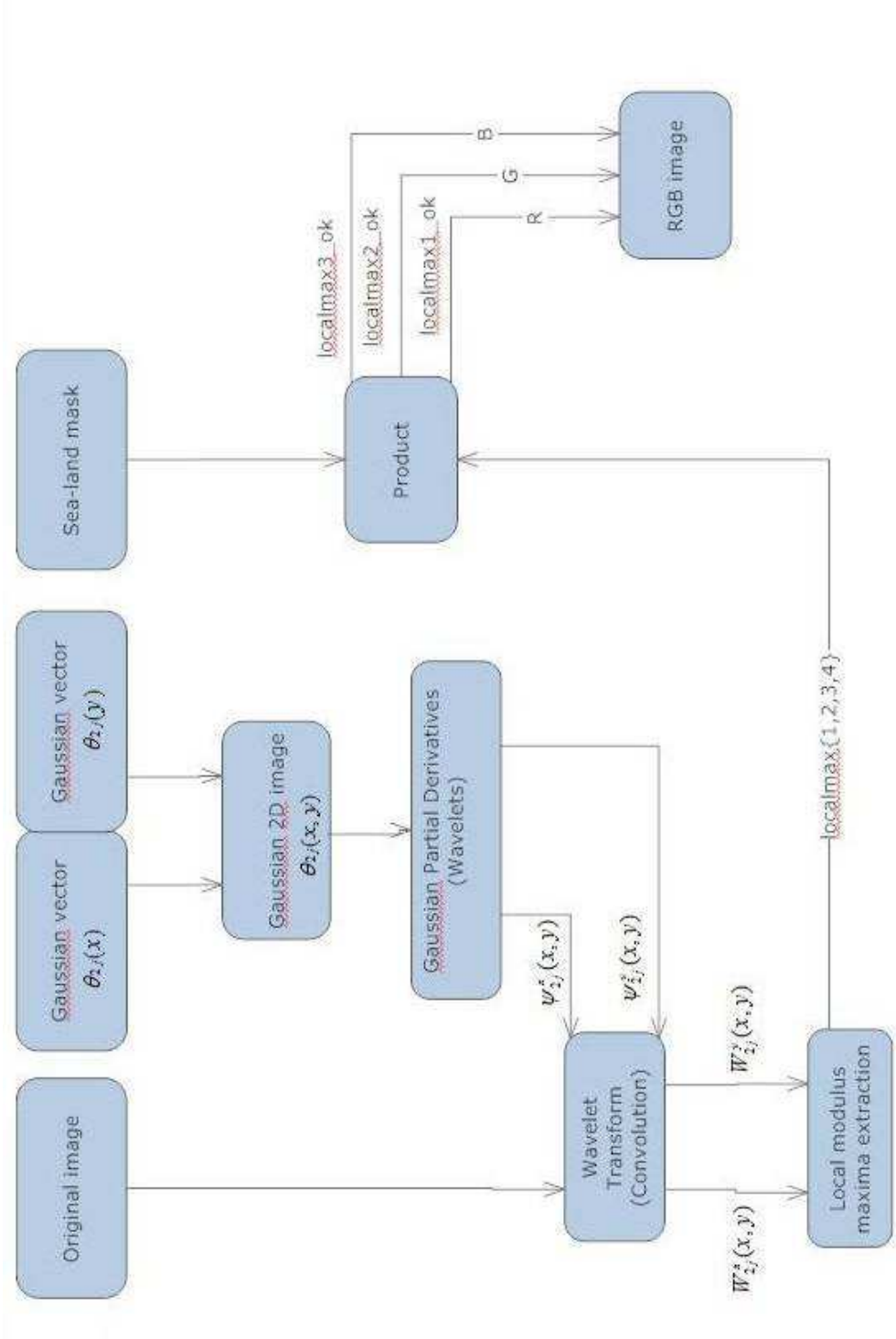

Figure 4.1.1 Block diagram of the implemented algorithm

4.2. Sea and land separation

In the proposed method the first step would be the coastline detection. For this work it is taken into account that ocean areas in SAR images are much more homogeneous than land areas, and features reflecting the 'roughness' of an image can be very useful. This part of the project has been done following the technique proposed in [Ref. Dellepiane.] and it will not be explained in detail since it is not the aim of this project.

The masks that are achieved with this technique have the same size as the image, and have a value of zero in the area corresponding to land and a value of one in the area corresponding to the sea.

This way it will be multiplied by the original image or by the original image processed in the most suitable moment of the algorithm. The most suitable moment to execute this operation will be the one that produces the best results.

Before computing the local modulus maxima images, it is necessary to apply some processing to the sea-land separation mask. That is because the sea-land separation edge is considerably stronger than edges created by waves or current changes and when calculating the local modulus maxima it could seem that the sea-land edge is a oceanic feature.

To avoid this the mathematical morphology have been used, concretely the erosion operation.

The erosion of the binary image *A* by the structuring element *B* is defined by:

$$A \ominus B = \{z \in E | B_z \subseteq A\},$$

where B_z is the translation of *B* by the vector z, and E is the result of the erosion.

$$B_z = \{b + z | b \in B\}, \forall z \in E.$$

When the structuring element *B* has a centre (e.g., *B* is a disk or a square), and this centre is located on the origin of *E*, then the erosion of *A* by *B* can be understood

as the locus of points reached by the centre of *B* when *B* moves inside *A*. [Ref Rafael C.Gonzalez, Richard E. Woods]

4.2 Wavelet masks generation

In order to define the wavelet masks we will use the partial derivatives of a Gaussian 2D image, which is a smoothing function. To get these 2D Gaussian images we follow the next reasoning:

It is proposed to generate a two dimension Gaussian image. To reach this goal, a Gaussian vector is generated. It is important to take into account the length of this vector and the variance of the Gaussian. The longer the length it is, the bigger neighbourhood will be considered.

The size of the Gaussian vector depends on the scale. The scale defines the size of the neighbourhood where the signal changes are computed. First, it is necessary to define the scale that corresponds to the analysis of the smallest neighbourhood. We will call fourth scale to that one. Besides, it is essential that the Gaussian vector has an odd number of elements as it is needed to have a pixel in the centre of the 2D Gaussian because it will be used to do a convolution.

The variance of a Gaussian defines its dispersion. In the case of an image, it defines the distance from the white centre of the image to the black or darker gray level of the perimeter. The higher is the variance value, smoother is the edge detection, since the mask changes its gray level smoothly.

Understanding the meaning of the variance in a Gaussian mask, it is very intuitive to realise that all the scales cannot have the same variance, since then, the unique difference between scales would be the quantity of black pixels added from the standard deviation to the size of the Gaussian. In the Figure 4.2.1 it is shown an example of the difference between two gaussian masks of the same size and different variance. The parameter σ is the standard deviation which is the square root of the variance.

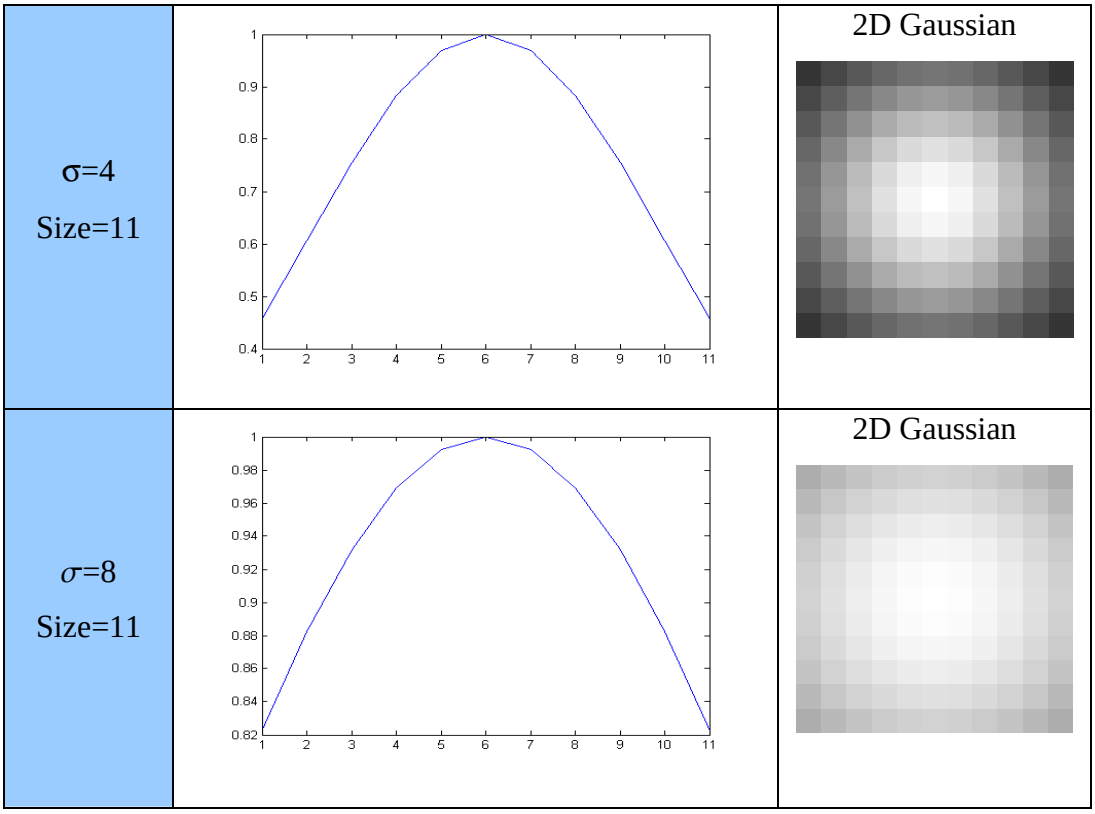

Figure 4.2.1 Comparative of the Gaussian variance values.

A Normal or Gaussian distribution follows the following equation:

$$f(x) = \frac{1}{\sqrt{2\pi\sigma^2}} e^{-\frac{(x-\mu)^2}{2\sigma^2}}$$

where σ^2 denotes the variance and μ the mean value.

A vector with Gaussian values is done in the abscissa direction, we will call it θ(x), and then we calculate the transpose of it, θ(y) that would correspond to a Gaussian vector in the ordinates direction. It is very intuitive to understand that by multiplying θ(x) and θ(y) we can obtaine the 2D Gaussian θ(x,y);

$$\theta(x, y) = \theta(x)\theta(y)$$

Once the 2D Gaussian image in the fourth level is obtained we calculate the third, the second and the first level of Gaussians. The size of the third level would be two times the size of the fourth level plus one to make sure that there is a pixel in the centre of the image and the next levels would be calculated in the same way.

The next step would be to calculate the partial derivatives of this 2D Gaussians. Therefore we define 2 oriented wavelets that will be:

$$\psi^1(x,y) = \frac{\partial\theta(x,y)}{\partial x} \quad \text{and} \quad \psi^2(x,y) = \frac{\partial\theta(x,y)}{\partial y}$$

These derivatives are calculated in the four levels.

4.3 Wavelet Transform

In order to get the Wavelet Transform of the image there will be used the two oriented wavelets calculated before. The partial derivative with respect to *x* will detect the horizontal edges and the derivative with respect to *y* will detect the vertical ones.

To perform this operation is it used the convolution. It is defined as follows:

$$W_{2^j}^1(x,y) = f(x,y) * \psi_{2^j}^1(x,y) = \int_{-\infty}^{\infty}\int_{-\infty}^{\infty} f(\alpha,\beta)\psi_{2^j}^1(x-\alpha, y-\beta)d\alpha d\beta$$

$$W_{2^j}^2(x,y) = f(x,y) * \psi_{2^j}^2(x,y) = \int_{-\infty}^{\infty}\int_{-\infty}^{\infty} f(\alpha,\beta)\psi_{2^j}^2(x-\alpha, y-\beta)d\alpha d\beta$$

Taking into account the convolution properties with the differentiation:

$$\begin{pmatrix} W_{2^j}^1 f(x,y) \\ W_{2^j}^2 f(x,y) \end{pmatrix} = 2^j \begin{pmatrix} \frac{\partial}{\partial x}(f * \theta_{2^j})(x,y) \\ \frac{\partial}{\partial y}(f * \theta_{2^j})(x,y) \end{pmatrix} = 2^j \nabla (f * \theta_{2^j})(x,y)$$

Where k=1 and k=2 describes the direction of the wavelet and 2^j denotes the scale.

4.4 Modulus Local maximums

The multiscale edge representation is built on the multiscale gradient representation. For this purpose, it is convenient to represent the multiscale gradient in magnitude-angle pairs, where the magnitude and angle are defined at each scale by:

$$M_{2^j} f(x,y) = \sqrt{\left| W_{2^j}^1 f(x,y) \right|^2 + \left| W_{2^j}^1 f(x,y) \right|^2}$$

$$A_{2^j} f(x,y) = \arctan\left[\frac{W_{2^j}^2 f(x,y)}{W_{2^j}^1 f(x,y)} \right]$$

For each scale 2^j, we collect the edge points along with the corresponding values of the gradient (i.e., the WT values) at that scale. This process is done following the Non-maximum suppression method. This is often used along with edge detection algorithms. The image is scanned along the image gradient direction, and if pixels are not part of the local maxima they are set to zero. This has the effect of suppressing all image information that is not part of local maxima.

Let denote d1, d2, d3 and d4 the four basic edge directions discussed for a 3x3 region: horizontal,-45 degrees, vertical and +45 degrees, respectively. The nonmaxima suppression scheme for a 3x3 region centered at every point (x,y) in Af(x,y) (the phase) is formulated as follows [Ref Rafael C.Gonzalez, Richard E. Woods]:

- Find the direction d_k that is closest to Af(x,y).
- If the value of the modulus at (x,y) is less than at least one of its two neighbours along d_k, let set this pixel to zero, otherwise, it will be set to the value of the modulus at this point.

At this point it will be obtained an image for each scale with the nonmaxima edge points suppressed.

The work done until now could be replaced by the Canny algorithm which follows basically the same process.

4.5 Multiresolution image fusion

At fine scales, there are many modulus maxima created by the image noise and the light textures. At large scales, the modulus maxima created by the noise and texture have disappeared and only the important edges remain.

In order to integrate the information contained in the four scales I have been proving a lot of methods.

The first idea was to multiply the four scales, this way the pixels in which the scales were similar will be brighter. With this method the final image had lost all the interesting information.

The next attempt was based on the morphological processing. Applying a dilation to the local modulus maxima images at different scales, the information contained in them is clearer.

Finally, a RGB image is created. In each of its channels a different level local modulus maxima is inserted. In the R channel will be the first level local maxima, in the G the second's level local maxima and in the B the third's one.

With this method the information is not lost as in the product method, and the visualization is easier.

At this point a study of the colour of the pixels is performed.

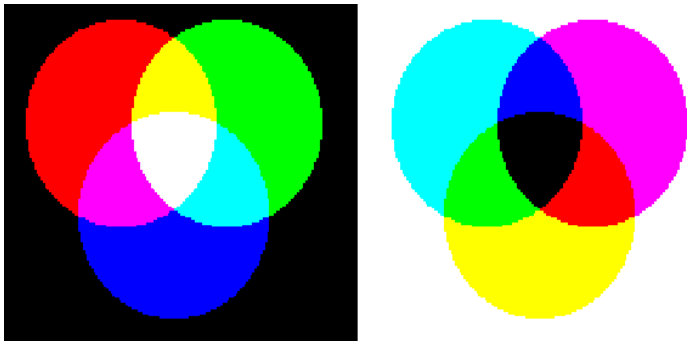

Figure 4.5.1 The RGB (red,green,blue) color model and its negative, the CMY (cyan, magenta yellow)

The results wil be shown in both models, the RGB and the CMY. When a pixel has a high value in the three components R, G and B, it will be white. Therefore, a white pixel in the RGB image, will mean that in this pixel there is a local modulus maxima in the first three levels, in other words, there is an edge. In the images which this project is based on, a white pixel will mean an internal wave. By introducing the first three levels in the RGB channels it is possible to see the real edges and to discard the local modulus maxima created by the noise.

The images will be shown also in the CMY representation because of its clarity . It is the negative of the RGB model and it is calculated as:

$$\begin{pmatrix} C \\ M \\ Y \end{pmatrix} = \begin{pmatrix} 1 \\ 1 \\ 1 \end{pmatrix} - \begin{pmatrix} R \\ G \\ B \end{pmatrix}$$

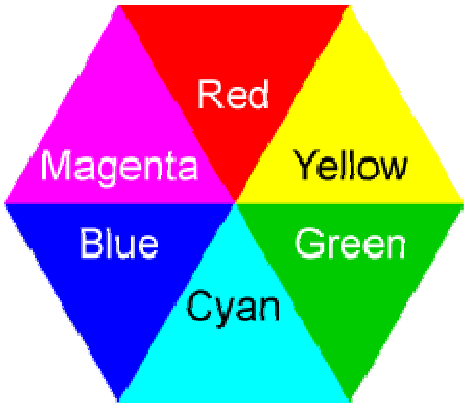

Figure 4.5.3 Complementary colours

The relevant information will be corresponding to the white in the RGB model and to the black in the CMY model

.

5) RESULTS

5.1. Dataset Tuscany

This tesis has been developed using three SAR images. These images have been captured by the COSMO Skymed satellite of the ASI (Agenzia Spaziale Italiana) in the region of Tuscany (Italy). The acquisition method was Stripmap, that is, each pixel covers a zone of 2’5 metres.

Figure 5.1.1 Image1. Satellitary SAR image acquired the 4th January of 2010 in Piombino (Tuscany). It has a size of 3000x3000 pixels.

Figure 5.1.2 Image 2. Satellitary SAR image acquired the 5th January of 2010 in Piombino (Tuscany). It has a size of 3000x3000 pixels.

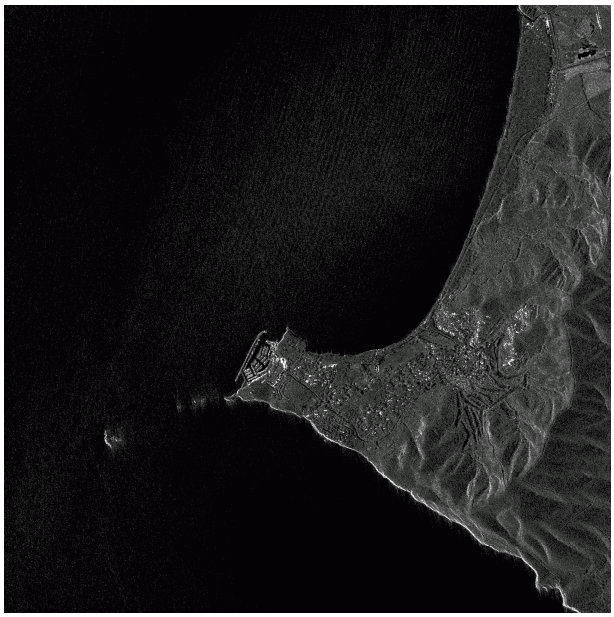

Figure 5.1.3 Image 3. Satellitary SAR image acquired the 5th January of 2010 in Punta Ala (Tuscany). It has a size of 3000x3000 pixels.

5.2. RESULTS

In this chapter the intermediate and final results of the implemented algorithm will be expounded and commented.
The implemented functions will be explained with their corresponding inputs and outputs. The function that includes all the processing is called detect_waves .

```
[rgb_image]=detect_waves(i,mask)
```

It needs an image and its sea-land separation mask and it returns a RGB image where the white pixels are those corresponding to the waves.

5.2.1 Gaussian 2D images

To get these 2D Gaussian images, a function called *teta* is used. The inputs of that function are *sigma*, the standard deviation and *size*, the number of elements of the Gaussian vector, and the output is *gaussian2d*.

```
[gaussian2d]=tita(sig,size)
```

This function is called in the main one, four times, as they are needed four different masks.
The scale which takes into account the smallest neighbourhood is the fourth one and its Gaussian is formed with five element vectors. The third level's size is eleven, the second's twenty three and the first's forty seven.
The mask's size is a very important parameter since the images which I am working with have a size of 3000x3000 pixels, and the dark and bright lines of the waves will have the corresponding size, so with a small mask the waves are not seen.

It is important to note that the variance must be changed in each level. If it is not done, there will not be difference between different levels.

That's why in the fourth level I have chosen a sigma =4, and in each following level the double of the precedent level.

The appearance of these 2D Gaussian images in the four levels is shown below:

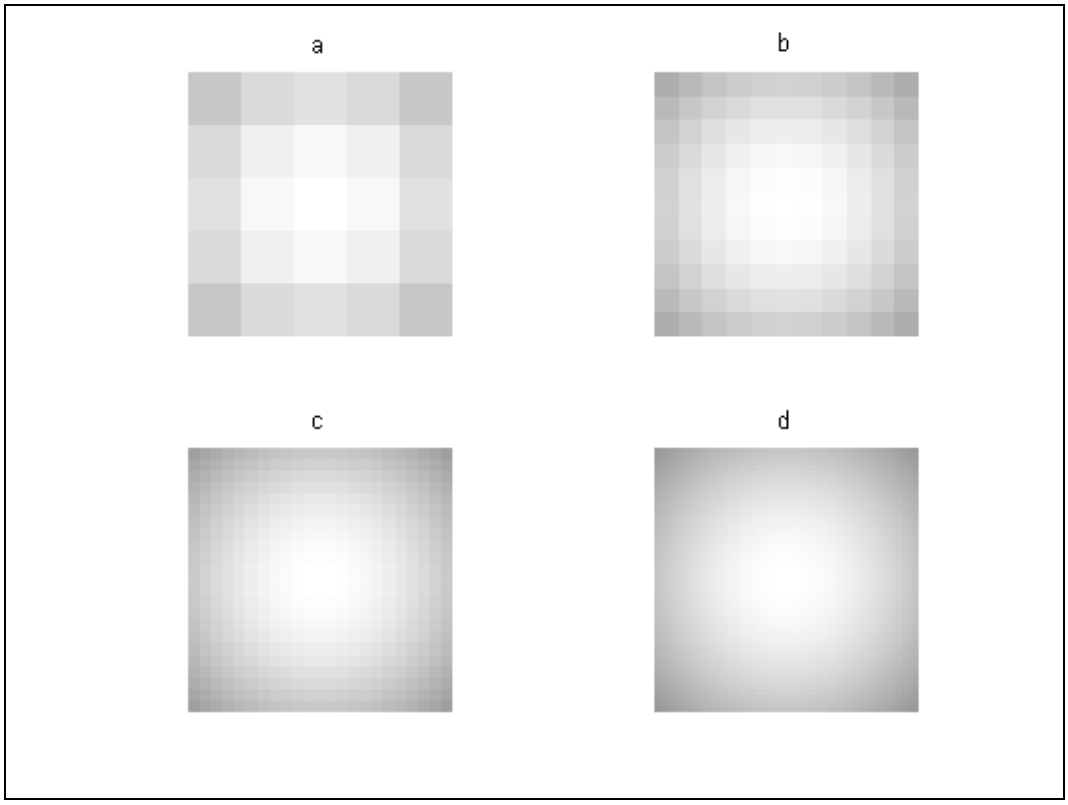

Figure 4.2.1 Gaussian images: a) The size of the mask is 5x5 and the variance 4^2, b) The size of the mask is 11x11 and the variance 8^2, b) The size of the mask is 23x23 and the variance 16^2, b) The size of the mask is 47x47 and the variance 32^2.

Calculating the partial derivatives of these Gaussians we get two images in each level corresponding to the two different directions.

The function to implement the partial derivatives:

```
[fix,fiy,s,l]=fi(teta,long)
```

Teta is the 2D Gaussian and *long* is the size of *teta*. The outputs are the two partial derivatives and *s* and *l*, two integer values that define the minimum and the maxima of the derivatives. These values are needed because the derivatives have negative values and it is necessary to do a stretching in order to represent them in a good way.

To compute them it is used the matlab's *diff* function. As the *diff* function dimensions the image removing a row or a column depending on the direction of the derivative, in order to get images with the same size as the original Gaussian I have duplicated the last row or column. The other choice was to add a zero's row or column but this way seems to differentiate more from the reality.

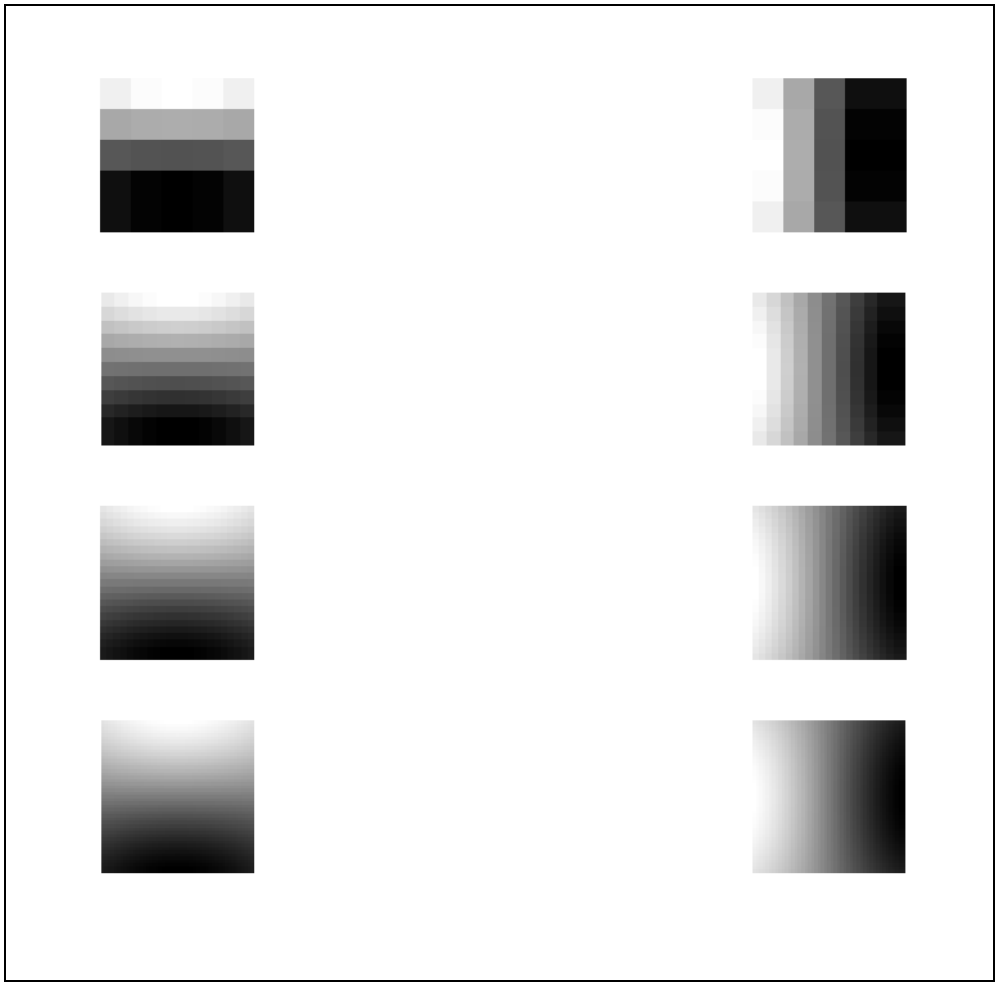

Figure 4.2.4 Partial derivatives. The first line corresponds to the fourth level and the last one to the first. In the left column are the partial derivatives with respect to *x* and in the right column are the partial derivatives with respect to *y*.

5.2.2 Wavelet Transform

Once I get the partial derivatives in the four levels I proceed to convolve them with the original image. As it is well known, the convolution operation makes the size bigger. In order to avoid it, I have used the matlab function *conv2* with the property of *'same'*.

I have been using different mask sizes. In the images below there is the comparison in the first level of the first image using a mask for the fourth level of five pixels, eleven pixels, and a twenty three pixels. Note that these images are not binary, they also have negative values.

	Fourth level	Third level	Second level	Third level
First prove	5	11	23	47
Second prove	11	23	47	95
Third prove	23	47	95	191

There will be shown the first level's results in each prove since it is the clearest level.

First prove:

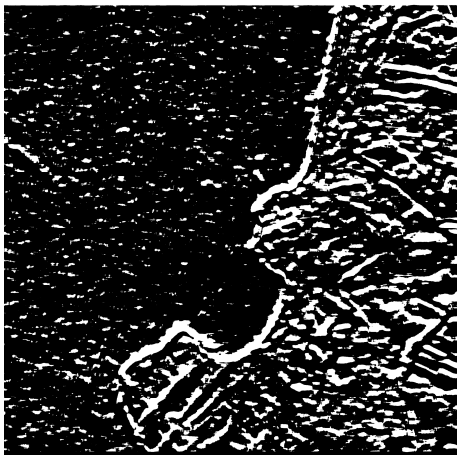

Figure 5.3.1 w1x

Figure 5.3.2 w1y

Second prove:

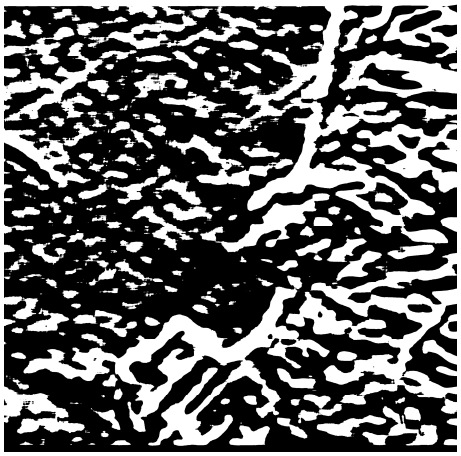

Figure 5.3.3 w1x

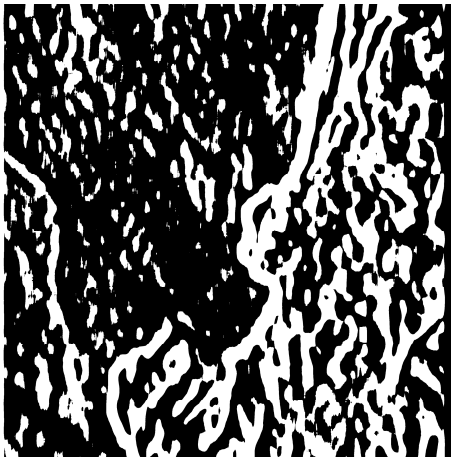

Figure 5.3.4 w1y

Third prove:

Figure 5.3.5 w1x

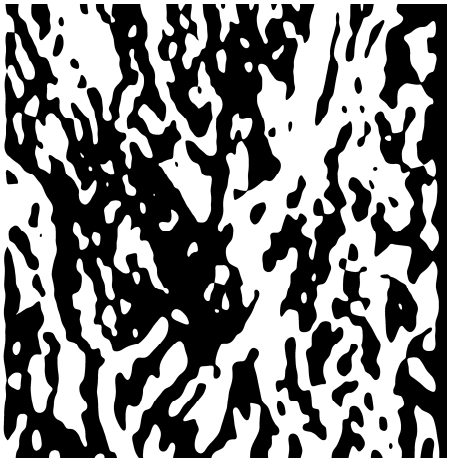

Figure 5.3.6 w1y

As it can be seen in the previous images the size of the mask is really important in order to detect the different ocean features.

The size of the mask that better fits the aim of this project is the used in the third prove.

Once the size of the mask is the most suitable, I proceed to obtain the Wavelet Transform in the four levels of the rest of the images .

In the images below can be seen how those which have been obtained convolving with a vertical mask, partial derivative with respect to y, bring out the vertical edge, and those which have been obtained convolving with a horizontal mask bring out the horizontal edges.

It can also be seen that by the way the used mask is smaller, and in the same way the scale, the fine details are shown instead of the big contrast zones. That is because of the smaller masks take into account only the closest neighbourhood.

Image 1

As the First level of this image has been previously shown I will start expounding the second one.

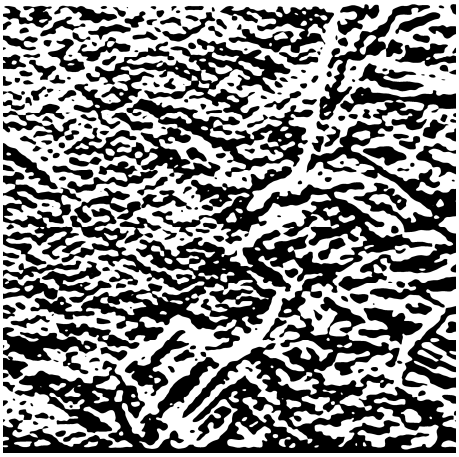

Figure 5.3.7 w2x

Figure 5.3.8 w2y

Figure 5.3.9 w3x

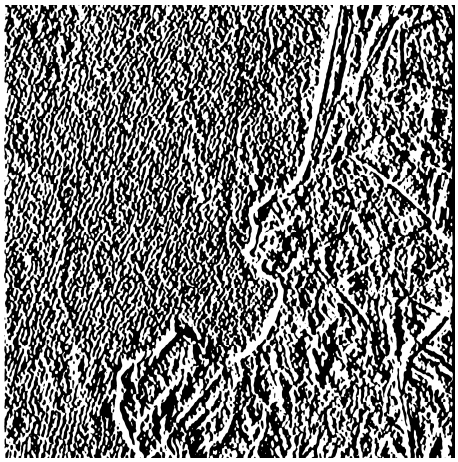

Figure 5.3.10 w3y

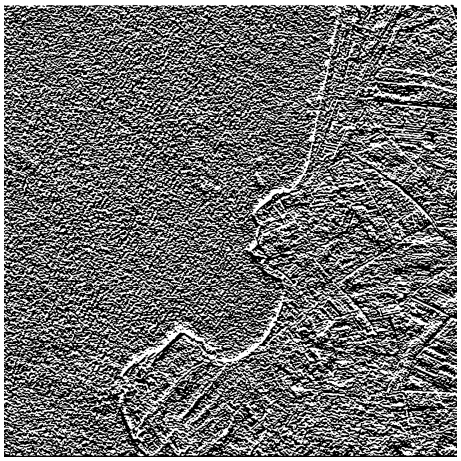

Figure 5.3.11 w4x

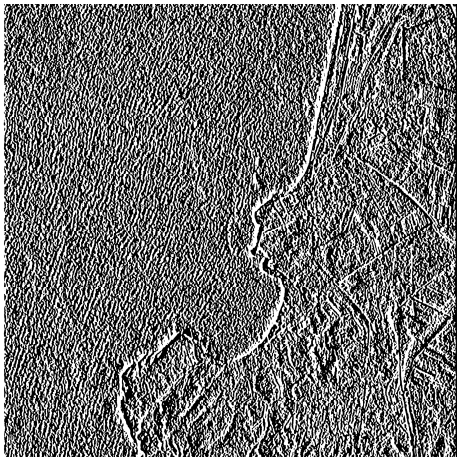

Figure 5.3.12 w4y

Image 2

For this image, will be just shown the first and the second levels.

Figure 5.3.11 w1x

Figure 5.3.10 w1y

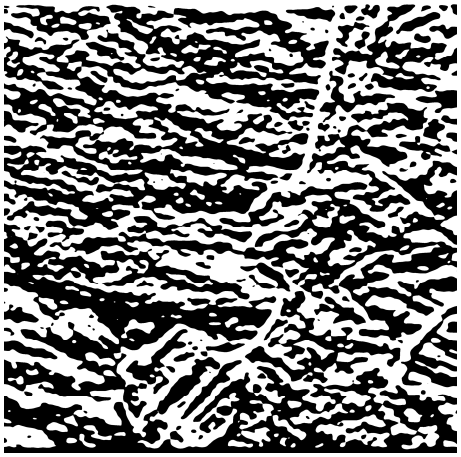

Figure 5.3.13 w2x

Figure 5.3.14 w2y

Image 3

As well as for the second image, it will be shown the most relevant resolution levels, that is the first and the second.

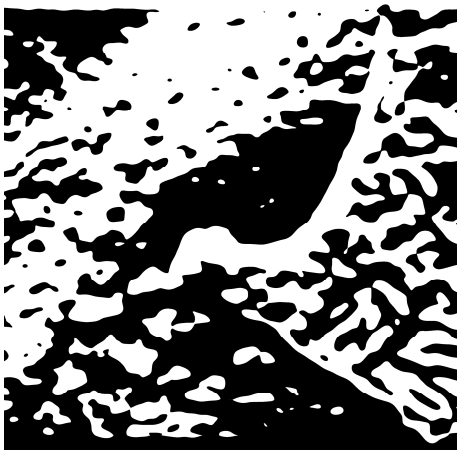

Figure 5.3.15 w1x

Figure 5.3.16 w1y

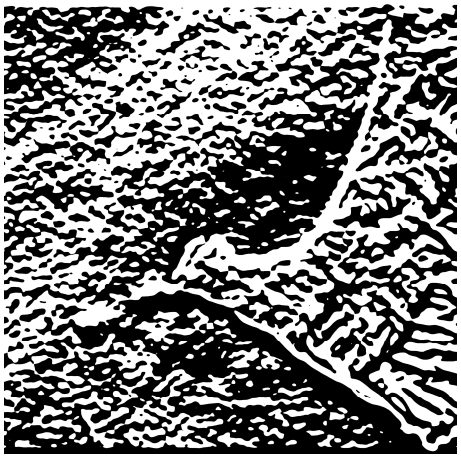

Figure 5.3.17 w2x

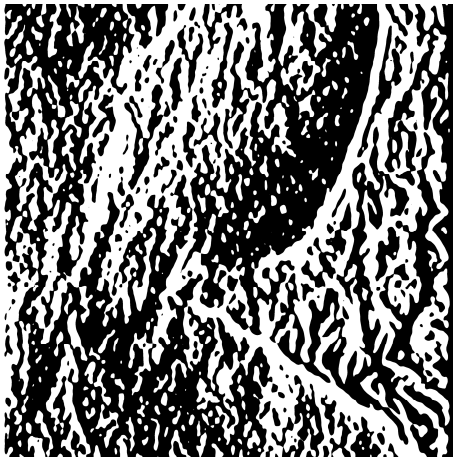

Figure 5.3.18 w2y

The mask of the land-sea separation hasn't been still used because if I apply it before finding the local maxima the most detected edges will be the ones of the separation line.

5.2.3 Mask adjustment

Before computing the local modulus maxima images, it is necessary to apply some processing to the sea-land separation mask. That is because the sea-land separation edge is considerably stronger than edges created by waves or current changes and when calculating the local modulus maxima it could seem that the sea-land edge is a oceanic feature.

To avoid this, it has been used the mathematical morphology, concretely the erosion operation.

The structuring element has been a circle with the same radius as size of the mask in the first resolution level.

Figure 5.2.3.1 Original sea-land separation mask

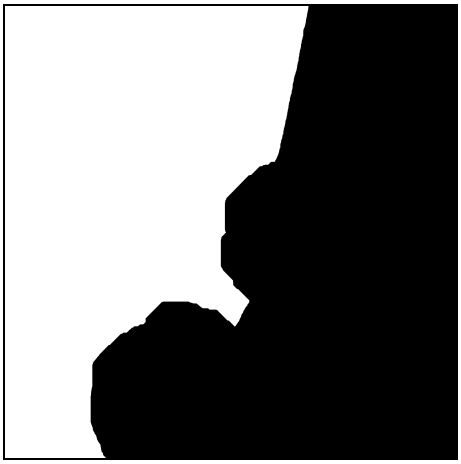

Figure 5.2.3.2 Eroded mask

5.2.4 Local modulus maxima

The next task is based on finding the local modulus maxima. That is, the two images that have been calculated before in each level, one on the ordinates direction and the other on the abscises direction, form the gradient.
The local modulus maxima would correspond to the maxima of the modulus along the direction of the angle.

```
[localmax]=max_modulus(wx,wy)
```

Sending the two wavelet transforms to *max_modulus* we get a matrix (image) with the wavelet maxima.
To implement that, we proceed to a method similar to the well known *non maximal suppression*. The calculated angle is discretized into 4 directions. For each direction the values of the modulus in that direction are interpolated. If the values confirm that there is an edge in that direction, the value of the modulus in that point is preserved, if not it will be set to zero.

That way we get four images, of the four levels wavelet maxima.
Since these images have really poor contrast I have proved to dilate those images in order to visualize them in a better way .
The function that improves the visibility of the local maxima images is:

```
[d1,d2,d3]=dilation_levels(localmax1_ok,localmax2_ok,localmax3_ok)
```

Its inputs are the local maximums of the three first levels and the output are those images dilated with a 25x25 square.
In the next images is shown the local modulus maxima of the first scale of the three images I have been working with.

Image 1

Figure 5.2.4.1 Original local modulus maxima image's negative.

.

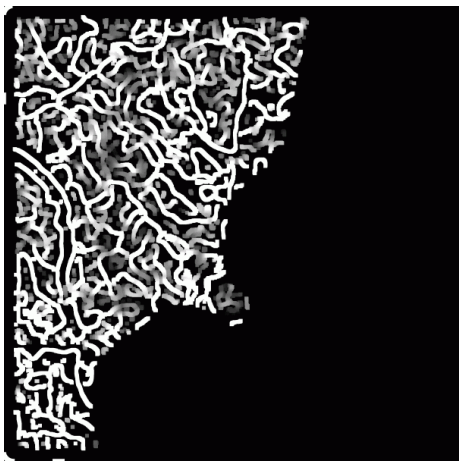

Figure 5.2.4.2 Local modulus maxima image dilated with a 25x25 square

Image 2

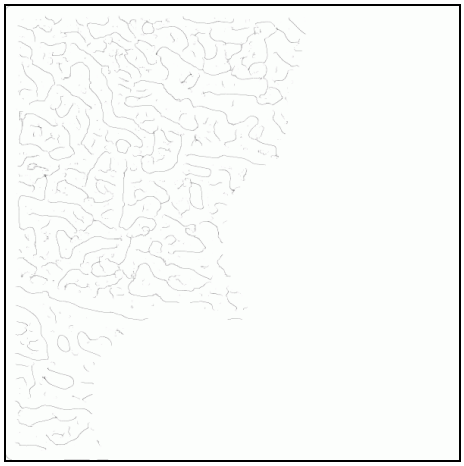

Figure 5.2.4.3 Original local modulus maxima image's negative.

.

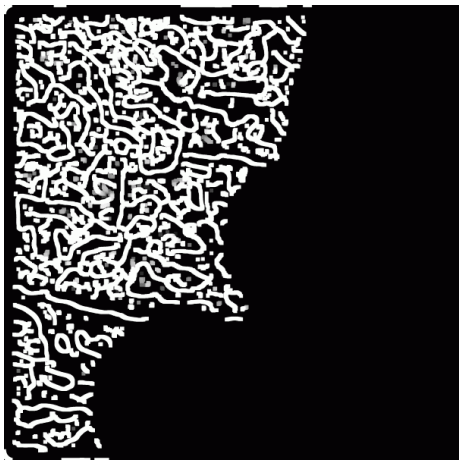

Figure 5.2.4.4 Local modulus maxima image dilated with a 25x25 square

Image 3

Figure 5.2.4.5 Original local modulus maxima image's negative.

.

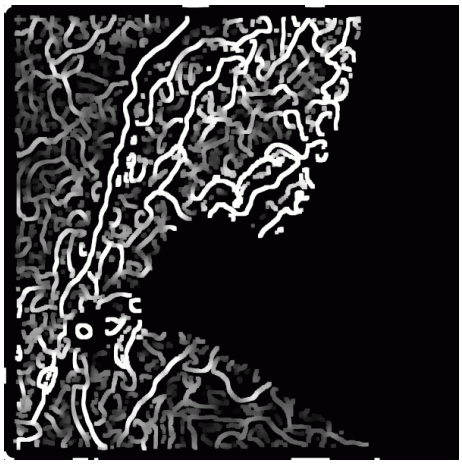

Figure 5.2.4.6 Local modulus maxima image dilated with a 25x25 square

5.2.5 Scale fusion

As it is previously explained, the methodology used to integrate the information contained in the different scales will use the RGB model.
The function that fusions the three first levels into a single RGB image is:

```
[rgb_image]= rgb_converter(r,g,b)
```

It only needs the first three resolution levels of the dilated local maxima images and obtains a RGB image.
As it is explained in the methodology section the interpretation of the RGB image is given by the following table:

R	G	B	
H	L	L	RED
H	L	H	MAGENTA
H	H	L	YELLOW
L	H	L	GREEN
L	H	H	CYAN
L	L	H	BLUE
H	H	H	WHITE
L	L	L	BLACK

Table 5.2.5.1 Interpretation of the relation between differnet colours (RGB) and the level to which they come from .H=high, L=low.

The white features are the ones corresponding to the waves, because of the fact that white pixels imply to have a high value in the three colour components, this way the noise is discarded.

C	M	Y	
H	L	L	CYAN
H	L	H	GREEN
H	H	L	BLUE
L	H	L	MAGENTA
L	H	H	RED
L	L	H	YELLOW
H	H	H	BLACK
L	L	L	WHITE

Table 5.2.5.2 Interpretation of the relation between differnet colours (CMY) and the level to which they come from .H=high, L=low.

So, in the CMY images the pixels corresponding to waves will be black.

It has been observed that the largest white lines which are surrounded by blue are the corresponding to current changes, and the not very long chains of white pixels are just the waves.

Image1:

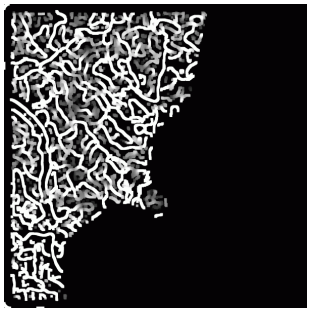

Figure 5.2.5.1

R: first level

Figure 5.2.5.2

G: second level

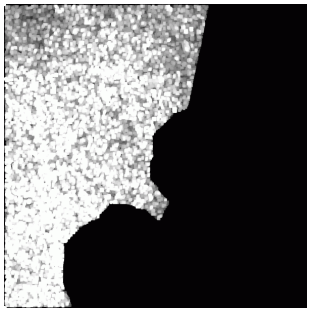

Figure 5.2.5.3

B:third level

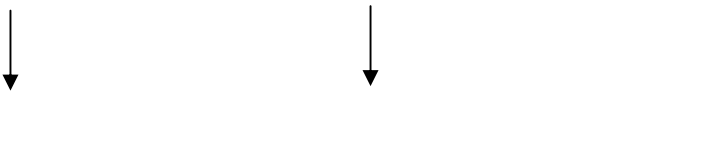

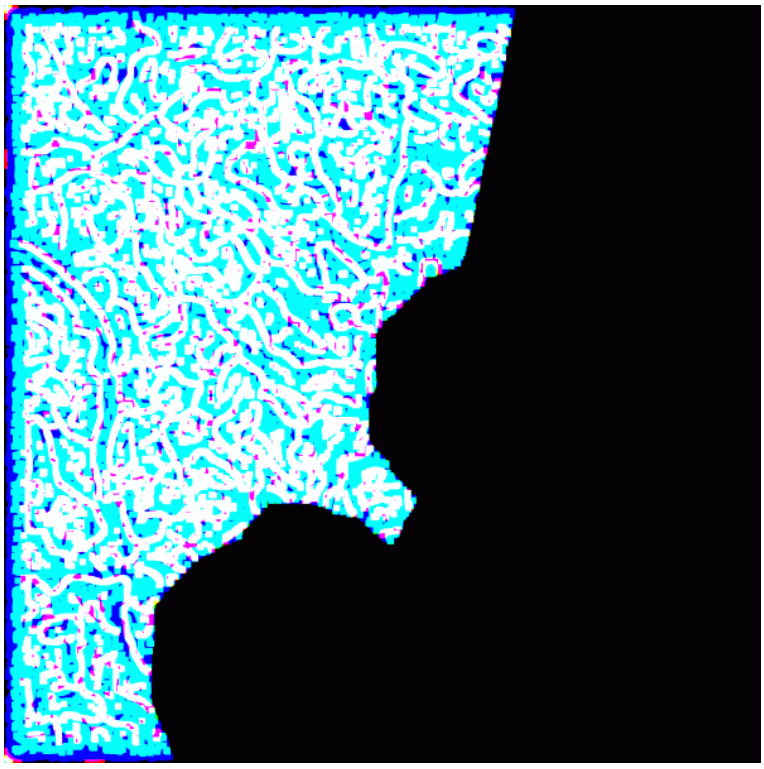

Figure 5.2.5.4 RGB image of the fusion of the three first levels of the Image 1.

In the case of the negative of the image it is easier to see the segmented waves and current changes.

Figure 5.2.5.5 Equalized image of the Image 1. It has been equalized in order to make visible the features to detect. The red circles denote that there are bright points in the original image, that are waves or current changes.

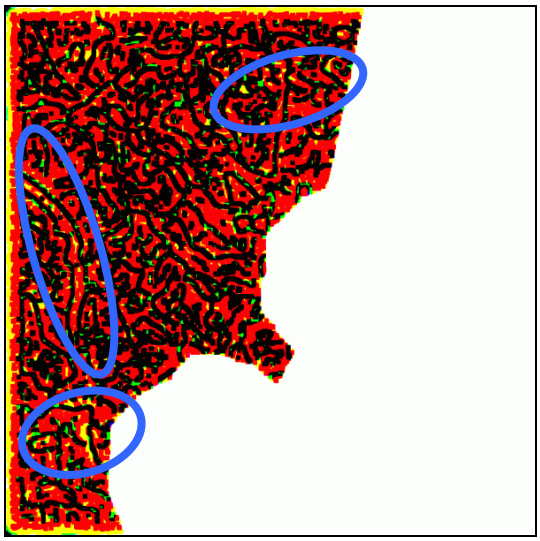

Figure 5.2.5.6 Negative of the RGB image. That is, CMY image. The important pixels are those black.

Image 2

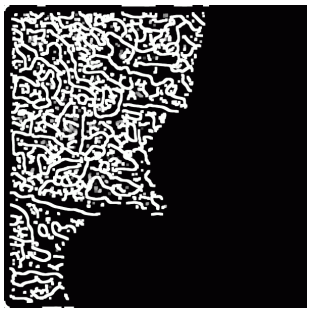

Figure 5.2.5.7
R: first level

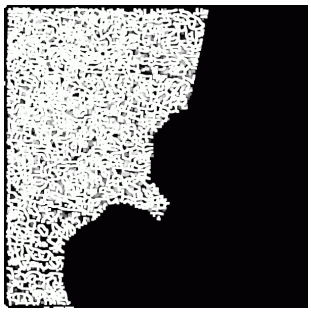

Figure 5.2.5.8
G: second level

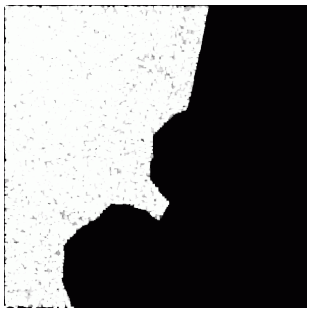

Figure 5.2.5.9
B:third level

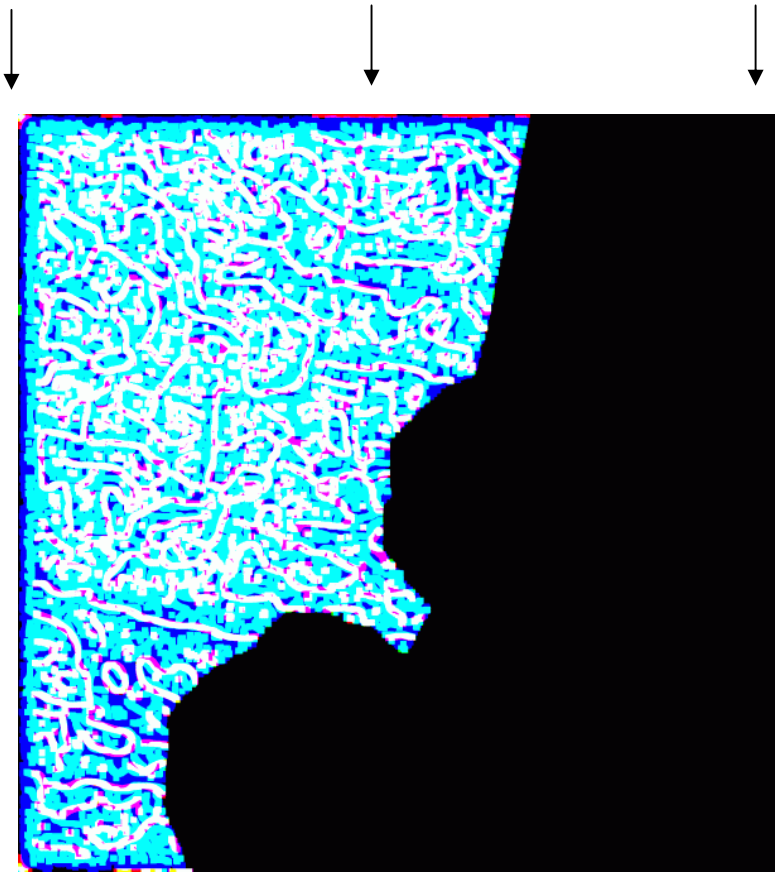

Figure 5.2.5.10 RGB image of the fusion of the three first levels of the Image 2.

Figure 5.2.5.11 Equalized image of the image 2. It has been equalized in order to make visible the features to detect. The red circles denote that there are bright points in the original image, that is waves or current changes.

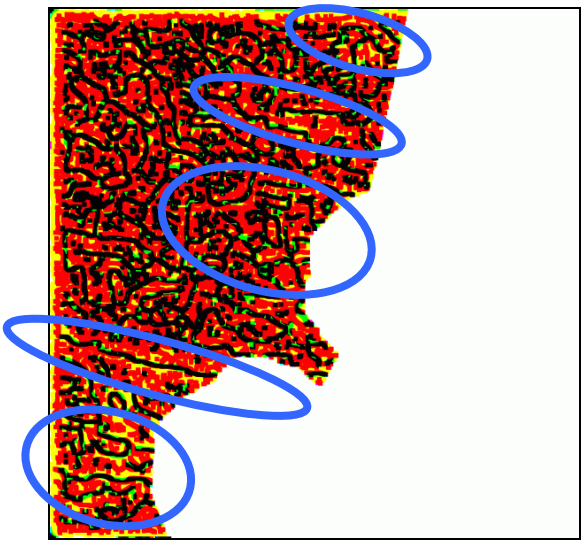

Figure 5.2.5.12 Negative of the RGB image. That is, CMY image. The important pixels are those black.

As it is previously commented the important current changes and waves appear in the RGB image as white large lines with some blue surrounding, and in the CMY image as large black lines with some yellow surrounding.

Image 3

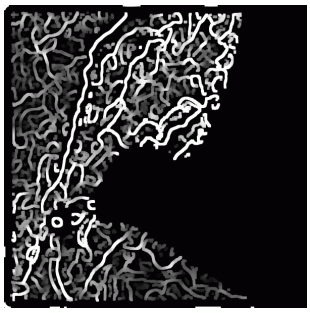

Figure 5.2.5.13

R: first level

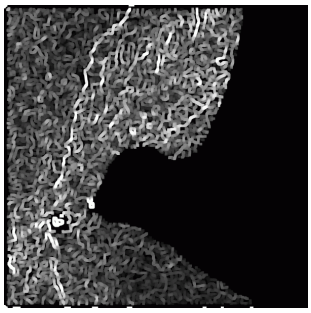

Figure 5.2.5.14

G: second level

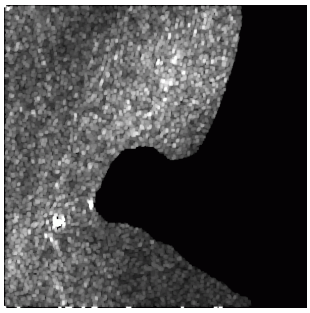

Figure 5.2.5.15

B:third level

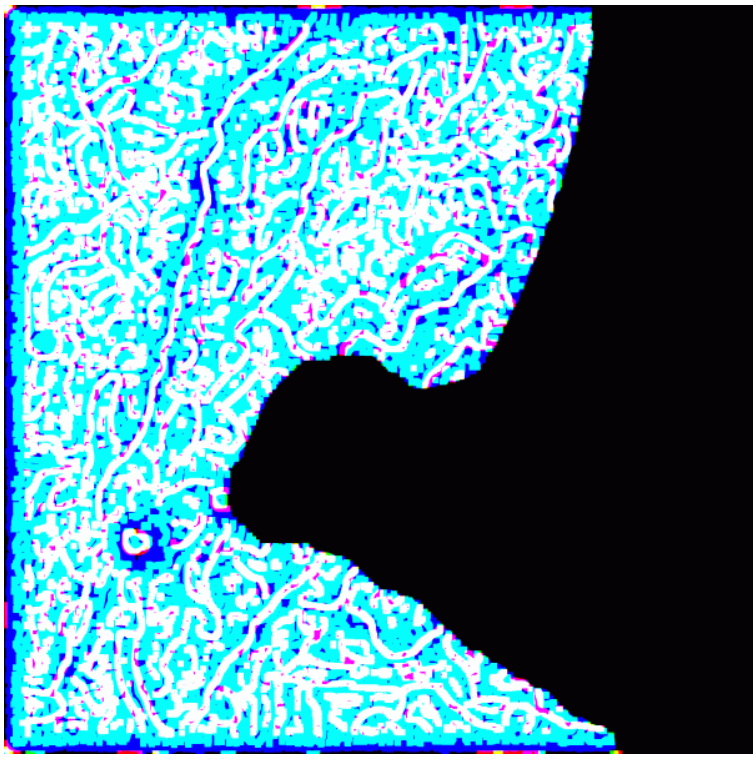

Figure 5.2.5.16 RGB image of the fusion of the three first levels of the Image 3.

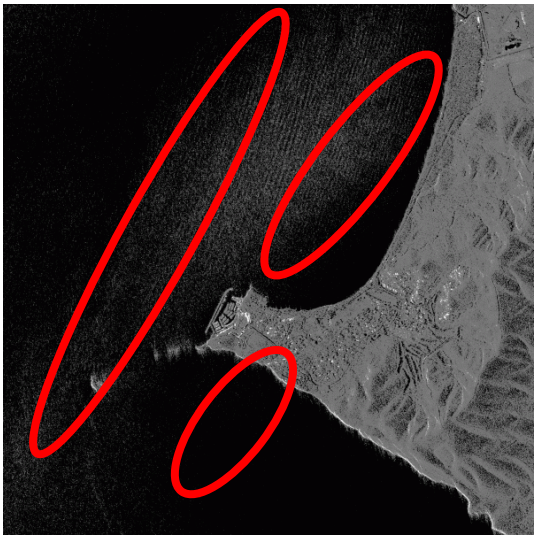

Figure 5.2.5.17 Equalized image of the image 3. It has been equalized in order to make visible the features to detect. The red circles denote that there are bright points in the original image, that is waves or current changes.

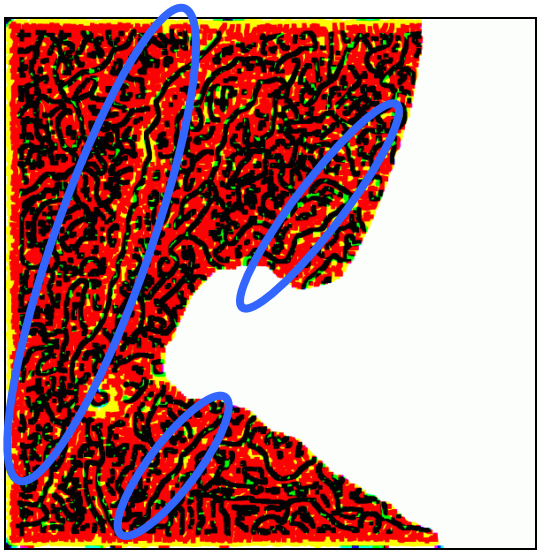

Figure 5.2.5.18 Negative of the RGB image. That is, CMY image. The important pixels are those black.

6 CONCLUSIONS

In this project it has been confronted the problem of detecting internal waves in SAR satellite images. The implemented algorithm has been applied in three SAR images. The method used to detect the edges that form the internal waves and the current changes has been based on the multiresolution processing and the wavelets although in the intermediate steps it has been necessary to use other processing methods such as mathematical morphology. Finally to solve the problem of fusing the information of different scale it has been used the RGB colour composition model.

Two oriented wavelets for each resolution scale have been generated, specifically the partial derivatives of a Gaussian 2D image. The differences between levels have been the size of the corresponding mask and the variance of the Gaussian original image. The variance is the measure of the width of the gaussian distribution.

Those masks have been applied through the convolution to get the wavelet transform images. For each level there are two wavelet transforms. On the one hand the one in which the horizontal edges are detected, and on the other, the one in which the vertical edges are detected.

For each level, these two wavelet transforms are merged using a non-maximal suppression processing. It is calculed the modulus and the phase of the gradient formed by the two images, and then the local modulus maxima along the direction of the phase are computed. One of the most detected edges is the one corresponding to the sea-land separation.

The sea-land mask is eroded using a circular structuting element. This way when multiplying by the previously obtained local modulus maxima we are avoiding that the most detected edge is the sea-line separation line.

After this operation, an image has been obtained for each resolution level in which the local modulus maximas of the sea zone are detected. As this information it is

not very clear to interprete, it has been aplied the morphological operation of dilation, with a structuring element of a square in order not to benefit any particular direction.

Once the information provided by the local modulus maxima has been clearly interpreted, the three first resolution levels have been fused. The fourth one has been discarded because of its quantity of noise.

To merge the three first levels, many methods have been used until the best results have been found. Finally it has been chosen to introduce each resolution level in a RGB image channel. These pixels that have a high value in the three channels have a very high probability for being real edges, that is, waves, and not noise. These pixels appear in white. In order to get a better representation of the obtained results, the RGB image is converted to a CMY model image. This way, the detected features appear in black.

Taking the work done in this thesis it could be possibe to continue it in order to do a further processing of the ocean internal waves. The future research could be to separate internal waves from internal look-alike detected features and to detect automatically the internal waves. Besides it would be interesting to extract some internal wave characteristics such as internal wave orientation and characterization. To reach this goal, recently a lot of studies that fusion the wavelet and multiresolution procesing with the Radon and Hough transforms have been presented. Morever, the speed of the waves could be measured by using the Doppler method

The current work here serves as a motivation and explanation for the ongoing work on the understanding of internal waves from satellite data.

REFERENCES

Warrick, Delaney "A Wavelet Localized Radon Transform Based Detector for a Signal with Unknown Parameters" IEEE 1996

Rodenas, Garello "Internal Wave Detection and Location in SAR Images using Wavelet Transform" IEEE 1998)

Zhou Changbao, Yang Jingsong, Huang Weigen, Fu Bin,Shi Aiqin, Li Donglin "Satellite SAR Remote Sensing of ocean internal waves" 1999

Marghany "Internal Wave Detection and Wavelength Estimation" IEEE 1999

Marghany "Digital elevation model of internal wave detection" IEEE 2000

J. C. Nieto Borge, S. Lehner, A. Niedermeier and J. Schulz-Stellenfleth "Detection of ocean wave groupiness from spaceborne synthetic aperture radar " JOURNAL OF GEOPHYSICAL RESEARCH, 2004

Biao Chen 1, Can Ding 2, Hai-ping Hou "Research on Detection of Internal Wave Area Based on Power Spectrum in SAR Image" IEEE 2008

Rafael C.Gonzalez, Richard E. Woods "Digital image processing" Pearson Education 2008

Lee-Lueng Fu Benjamin Holt "Seasat Views Oceans and Sea Ice With Synthetic-Aperture Radar" February 15, 1982

Dellepiane S., De Laurentiis R., Giordano F., “Coastline extraction from SAR images and a method for the evaluation of coastline precision”, Pattern Recognition Letters, vol.25, pp. 1461-1470, 2004